machines

MDPI

Article

The Existence of Autonomous Chaos in EDM Process

Peng Wang [1,*], Zhuo Wang [2], Lihui Wang [3], Bo-Hu Li [4] and Binxiu Wang [5]

[1] School of Information Engineering, Beijing Institute of Petrochemical Technology, Beijing 102617, China
[2] College of Mechanical and Electrical Engineering, Harbin Engineering University, Harbin 150001, China; wangzhuo_heu@hrbeu.edu.cn
[3] Department of Production Engineering, KTH Royal Institute of Technology, 11428 Stockholm, Sweden; lihuiw@kth.se
[4] School of Automation Science and Electrical Engineering, Beihang University, Beijing 100083, China; libohu@tsinghua.edu.cn
[5] School of Mechanical and Automotive Engineering, Qingdao University of Technology, Qingdao 266033, China; boshiwang@buaa.edu.cn
* Correspondence: 0020200015@bipt.edu.cn

Abstract: The dynamical evolution of electrical discharge machining (EDM) has drawn immense research interest. Previous research on mechanism analysis has discussed the deterministic nonlinearity of gap states at pulse-on discharging duration, while describing the pulse-off deionization process separately as a stochastic evolutionary process. In this case, the precise model describing a complete machining process, as well as the optimum performance parameters of EDM, can hardly be determined. The main purpose of this paper is to clarify whether the EDM system can maintain consistency in dynamic characteristics within a discharge interval. A nonlinear self-maintained equivalent model is first established, and two threshold conditions are obtained by the Shilnikov theory. The theoretical results prove that the EDM system could lead to chaos without external excitation. The time series of the deionization process recorded in the EDM experiments are then analyzed to further validate this theoretical conclusion. Qualitative chaotic analyses verify that the autonomous EDM process has chaotic characteristics. Quantitative methods are used to estimate the chaotic feature of the autonomous EDM process. By comparing the quantitative results of the autonomous EDM process with the non-autonomous EDM process, a deduction is further made that the EDM system will evolve towards steady chaos under an autonomous state.

Keywords: electrical discharge machining; deionization; autonomous chaos; Shilnikov

Citation: Wang, P.; Wang, Z.; Wang, L.; Li, B.-H.; Wang, B. The Existence of Autonomous Chaos in EDM Process. *Machines* **2022**, *10*, 252. https://doi.org/10.3390/machines10040252

Academic Editor: Gianni Campatelli

Received: 7 March 2022
Accepted: 29 March 2022
Published: 31 March 2022

1. Introduction

Electrical discharge machining (EDM), as an advanced manufacturing technology, has been widely applied in machining non-traditional materials and complex products [1,2]. An electrical discharge channel consists of anode erosion, cathode erosion, and a plasma channel. The entire discharge reaction involves complex chemical, physical, thermal, and electrical processes occurring simultaneously [3]. Considerable interest has developed in comprehending the dynamical evolution of the EDM process.

One of the main approaches to studying electrical discharge is based on the Liouville equation, from which a deterministic equation is deduced for a stochastic process. Within this context, DiBitonto et al. [4] and Patel et al. [5] proposed linear models for cathode erosion and anode erosion, respectively. Eubank et al. [6] made efforts in modeling the plasma formed in dielectric. It should be noticed that these models disregard the initial canonical correlation as well as the nonlinear characteristics in the EDM process.

Nonlinear phenomena such as fractals and chaos have been investigated in various electrical discharge processes. Teitsworth et al. [7] focused on the electrical breakdown process and observed oscillatory instabilities due to impurity impact ionization. Alisultanov and Ragimkhanov [8] obtained a fractional equation to explain the electron avalanche and

the instability in a non-self-maintained electrical discharge. Allagui et al. [9] studied the cathodic and anodic contact glow discharge process and pointed out that the DC voltages in the discharge regime undergo a transition from quasi-periodic to chaotic to quasi. An assumption is made that this kind of transition may be due to the highly nonlinear hydrodynamic features of a complex interaction. Braun et al. [10,11] experimented on electrical gas discharges and described the appearance of current oscillations that can develop to deterministically chaotic behavior. Zhang et al. [12] established a one-dimensional fluid mode to analyze nonlinear behaviors of the atmospheric pressure in electrode dielectric barrier discharges.

In EDM research, it is known that a turbulent state is natural for plasma [13–15]. From this point of view, much work has been concentrated on the dynamical change within different kinds of plasma. Cheung et al. [16,17] showed that a pulsed plasma system had period doubling and chaotic behavior and then identified that the intermittent route to chaos exists in a steady-state plasma system. Wilson and Podder [18] attempted to alternate regions of stability and instability of a DC glow discharge plasma. Lahiri et al. [19] summarized Wilson's results and indicated the presence of fractional Brownian motion in plasma. Nurujjaman et al. [20] made an interesting discovery that with increasing input energy, the plasma channel changes irregularly from a stable state to a chaotic state. Ohno et al. [21] made a conclusion that chaotic states can never been observed in the absence of a weak DC excitation. The limitation of their work is obvious, because the experiment only focused on plasma and failed to consider the electrical discharge process as a whole.

To study a typical EDM process, Han and Kunieda [22] first proved chaos existence in the location of electrical sparks. Aich and Banerjee [23] further extracted the inherent fractal features of a machined surface generated by EDM. Gatto et al. [24] attempted to describe the evolution of energy employed at one discharge event using the logistic map recursive equation. Zhou et al. [25] investigated one part of the EDM process and found that the "efficient process" is chaotic. Wang et al. [26] proposed their own interpretation on the chaos of the continuous discharging process. However, it should be noted that the micro-reaction of EDM involves four sub-stages, namely partial dielectric ionization, dielectric breakdown, plasma channel formation, and dielectric deionization [27]. The former three sub-stages belong to the normal machining process, and the dielectric deionization could be described as an ineffective but inevitable sub-process. The evolution of the deionization process is directly related to the performance of electrical discharge machining. Dielectric deionization happens at the discharge interval, and it is not a machining process, but a phase in which dielectric restores the insulating properties. The existence of deionization makes engineers realize that there must be enough time delay between the two electrical pulses to complete the deionization process. Hayakawa et al. [28,29] concluded that, in the EDM process, bubble expansion and material removal occurs not only in the discharge duration but also in the deionization duration. In other words, there exists a special autonomous dynamical process without external excitation in an EDM system. Earlier articles, focusing on the nonlinear mechanism of the electrical discharge process, neglected these specific characteristics of EDM and treated the EDM system as a non-autonomous system, which is a barrier to the realization of a precise EDM model. To better understand the dynamical behavior of EDM, our work focuses on finding the evidence of chaos existence in the autonomous process of EDM. In Section 2, a nonlinear self-maintained equivalent model is presented. We analyze the model with the Shilnikov bifurcation theory and reveal a mathematical threshold condition under which the EDM system may lead to chaos without external excitation. To validate this theoretical conclusion, in Section 3, we study the time series signals of the deionization process recorded in EDM experiments. The experimental results verify that there is autonomous chaos in the EDM process. In Section 4, we discuss the chaotic mechanism of the EDM system by comparing the quantitative results of both the autonomous and non-autonomous EDM processes.

2. Autonomous Chaotic Analysis

2.1. Equivalent Model of Autonomous EDM Process

It has been verified that discharge gap states have electrical behavior [30,31]. Figure 1 shows the mechanism of the autonomous EDM process. With the disappearance of the external power source, there persists a potential difference between anode erosion and cathode erosion, which can be described as an equivalent capacitance. The resistance effect can be observed in anode erosion and cathode erosion, as well as in plasma. Hence, the anode erosion and the cathode erosion have both a resistance property and an inductance property. This electrical behavior can be represented by a resistance–inductance series equivalent circuit model. With the start of the deionization process, electronics and positive ions bind and change their original orbits irregularly, which will generate an irregular electric field. The electromagnetic inertia of this electric field can be represented with the resistance–capacitance characteristic and may be considered as a nonlinear parameter.

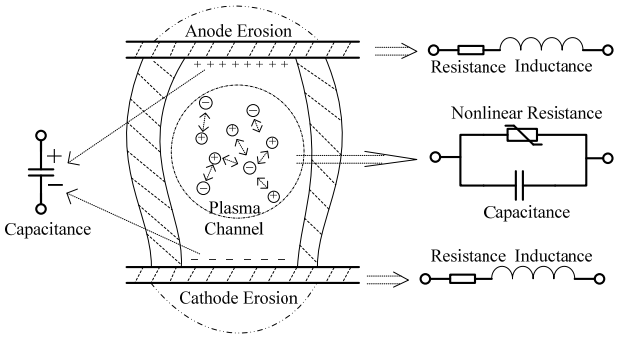

Figure 1. Autonomous EDM mechanism model.

The equivalent circuit model of the autonomous EDM process is shown in Figure 2. C_1 is the equivalent capacitance that represents the potential difference, R_1 and L_1 are the equivalent resistant and inductor that represent anode erosion, R_2 and L_2 are the equivalent resistant and inductor that represent cathode erosion. R_3 and C_2 in parallel connection represent a plasma channel. The voltage of C_2 is opposite to C_1, and R_3 could be considered as the nonlinear parameter. The volt–ampere relationship of non-linear resistors (NR) can be generally assumed as $i_{NR} = a_1 {u_{c_1}}^3 - a_2 u_{c_1} = g(u_{c_1})$, where $a_1, a_2 > 0$.

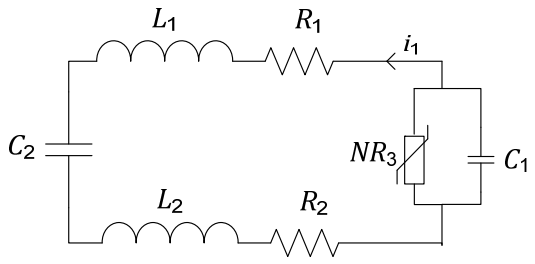

Figure 2. Equivalent model of autonomous EDM process.

Differential equations of the system are obtained by Kirchhoff's law as:

$$\begin{cases} -C_1 \frac{du_{C_1}}{dt} + g(u_{C_1}) = i_1 \\ (L_1 + L_2) \frac{di_1}{dt} = u_{C_2} - (R_1 + R_2) i_1 - u_{C_1} \\ C_2 \frac{du_{C_2}}{dt} = -i_1 \end{cases}, \quad (1)$$

Let $t = \left(\frac{L_1+L_2}{R_1+R_2}\right)\tau$, then $dt = \left(\frac{L_1+L_2}{R_1+R_2}\right)d\tau$. Equation (1) could be normalized as follows:

$$\begin{cases} -C_1\frac{R_1+R_2}{L_1+L_2}\frac{du_{C_1}}{d\tau} = i_1 - g(u_{C_1}) \\ L\frac{R_1+R_2}{L_1+L_2}\frac{di_1}{d\tau} = u_{C_2} - (R_1+R_2)i_1 - u_{C_1} \\ C_2\frac{R_1+R_2}{L_1+L_2}\frac{du_{C_2}}{d\tau} = -i_1 \end{cases}, \tag{2}$$

Let $x = -\frac{u_{c_1}}{R_1+R_2}$, $y = i_1$, $z = \frac{u_{c_2}}{R_1+R_2}$, $f(x) = g(-x(R_1+R_2))$, then we have:

$$\begin{cases} \frac{dx}{d\tau} = \frac{L}{C_1{R_1}^2}[y - f(x)] \\ \frac{dy}{d\tau} = x - y - z \\ \frac{dz}{d\tau} = -\frac{L}{C_2{R_1}^2}y \end{cases}, \tag{3}$$

Let $\alpha = -\frac{L_1+L_2}{C_1(R_1+R_2)^2}$, $\beta = -\frac{L_1+L_2}{C_2(R_1+R_2)^2}$, $f(x) = a_1(R_1+R_2)^3x^3 - a_2(R_1+R_2)x = cx^3 - dx$, where $c = a_1(R_1+R_2)^3$, $d = a_2(R_1+R_2)$.

Equation (3) can be rewritten as:

$$\begin{cases} \dot{x} = \alpha(y - f(x)) \\ \dot{y} = x - y + z \\ \dot{z} = -\beta y \end{cases}, \tag{4}$$

The above third-order autonomous system is defined as the model of EDM's deionization process.

2.2. Theoretical Analysis Based on Shilnikov Theory

The existence of chaos in Equation (4) could be justified by the heteroclinicShilnikov method [32]. To distinguish a chaotic system, the Shilnikov criteria are as follows:

1. There should be two distinct equilibrium points, denoted by x_e^1 and x_e^2, respectively, which of Equation (4) are saddle foci, whose characteristic values are γ_i,$\sigma_i \pm j\omega_i$, (i = 1,2);
2. There must be a heteroclinic orbit joining x_e^1 and x_e^2;
3. The system should satisfy the following Shilnikov inequality:

$$|\sigma_i/\gamma_i| < 1, \ (i = 1, 2), \tag{5}$$

where $\gamma_1\gamma_2 > 0$, or $\sigma_1\sigma_2 > 0$

We can find the equilibrium points $O_1(0,0,0)$, O_2, O_3 in Equation (4). Then, the Jacobian matrix corresponding to O_2, O_3 is:

$$A = \begin{bmatrix} -2\alpha d & \alpha & 0 \\ 1 & -1 & 1 \\ 0 & -\beta & 0 \end{bmatrix} \tag{6}$$

The characteristic equation of A could be written as:

$$\lambda^3 + (1+2\alpha d)\lambda^2 + (\beta - \alpha + 2\alpha d)\lambda + 2\alpha\beta d = 0 \tag{7}$$

Let $\lambda = \gamma - (1+2\alpha d)/3$, and the characteristic equation can be rewritten as:

$$\gamma^3 + P\gamma + Q = 0 \tag{8}$$

where $P = P(\alpha,\beta,d) = -\frac{(1+2\alpha d)^2}{3} + (\beta - \alpha + 2\alpha d)$, $Q = Q(\alpha,\beta,d) = \frac{2(1+2\alpha d)^3}{27} - \frac{(1+2\alpha d)(\beta-\alpha+2\alpha d)}{3} + 2\alpha\beta d$.

Define Δ as $\Delta = \left(\frac{P}{3}\right)^3 + \left(\frac{Q}{2}\right)^2$. As shown in the cubic root formula, if $\Delta > 0$, Equation (5) has a unique negative real root γ_1 and a pair of conjugate complex roots $\sigma_1 \pm j\omega_1$.

Considering theory one of the Shilnikov criteria, we can obtain $\left(\frac{P}{3}\right)^3 + \left(\frac{Q}{2}\right)^2 > 0$, and then the first threshold condition can be obtained as:

$$\beta - \alpha + 2\alpha d > \frac{(1 + 2\alpha d)^2}{3} \tag{9}$$

where α, β, d is directly related to L_1, L_2, C_1, R_1, R_2.

The next step is to find out whether there exists a heteroclinic orbit joining O_2, O_3.

Equation (4) can be transformed as:

$$\begin{aligned} y &= \tfrac{\dot{x}}{\alpha} + f(x) \\ z &= \tfrac{\ddot{x}}{\alpha} + \tfrac{\dot{x}}{\alpha} - x + f(x) + \dot{f}(x) \end{aligned} \tag{10}$$

From Equation (10), one can know that $x(t)$, $y(t)$, $z(t)$ can be determined with the value of $x(t)$.

To further simplify Equation (10), we can obtain:

$$\frac{d\left(\dddot{x} + \left(3\alpha c x^2 - \alpha d + 1\right)\dot{x} - (d+1)\alpha x + \alpha c x^3\right)}{dt} + \beta\dot{x} - \alpha\beta d x + \alpha\beta c x^3 = 0 \tag{11}$$

Now, the aim is to find an expression such that $x(t) = \varphi(t)$, satisfying Equation (11), as well as the following condition: if $t \to +\infty$, then $\varphi(t) \to -\sqrt{d/c}$, and $t \to -\infty$, $\varphi(t) \to \sqrt{d/c}$. Otherwise, if $t \to +\infty$, $\varphi(t) \to \sqrt{d/c}$, and $t \to -\infty$, $\varphi(t) \to -\sqrt{d/c}$.

Here, a definition could be first stipulated that $t \to +\infty, \varphi(t) \to -\sqrt{d/c}$. An assumption is made that: for $t > 0$,

$$\varphi(t) = -r + \sum_{k=1}^{\infty} \alpha_k e^{klt} \tag{12}$$

where $r = \sqrt{d/c}$, α_k $(k \in N^*, k \geq 1)$ and l are undetermined constants, $l < 0$.

Equation (12) can be substituted into Equation (11), and then the following result can be obtained:

$$\begin{aligned} &\sum_{k=1}^{\infty}\left[(kl)^3 + (2\alpha d + 1)(kl)^2 + (2\alpha d + \beta - \alpha)kl + 2\alpha\beta d\right]\alpha_k e^{klt} \\ &\quad - \sum_{k=2}^{\infty}\sum_{i+j=k}\left[3\alpha c r\left(2kl^2 i + kl + \beta\right)\alpha_i\alpha_j\right]e^{klt} \\ &\quad + \sum_{k=3}^{\infty}\sum_{i+j_1=k}\left[\alpha c\left(3kl^2 i + kl + \beta\right)\alpha_i\left(\sum_{m+n=j_1}\alpha_m\alpha_n\right)\right]e^{klt} = 0 \end{aligned} \tag{13}$$

where $(k, i, j, m, n, j_1) \in N^*$, $i \geq 1, j \geq 1$, $m \geq 1$, $n \geq 1$, $j_1 \geq 2$. As $e^{klt} \neq 0$ $(k \in N^*)$.

Comparing the coefficients of e^{klt}, for $k = 1$,

$$\left[l^3 + (2\alpha d + 1)l^2 + (2\alpha d + \beta - \alpha)l + 2\alpha\beta d\right]\alpha_1 = 0 \tag{14}$$

for $k = 2$,

$$\left[(2l)^3 + (2\alpha d + 1)(2l)^2 + (2\alpha d + \beta - \alpha)(2l) + 2\alpha\beta d\right]\alpha_2 = 3\alpha c r\left(4l^2 + 2l + \beta\right){\alpha_1}^2 \tag{15}$$

for $k \geq 3$,

$$\begin{aligned}&\left[kl^3 + (2\alpha d + 1)kl^2 + (2\alpha d + \beta - \alpha)lk + 2\alpha\beta d\right]\alpha_k \\ &= \sum_{i+j=k}\left(3\alpha cr\left(2kl^2 i + kl + \beta\right)\alpha_i\alpha_j - \sum_{i+j_1=k}\alpha c\left(3kl^2 i + kl + \beta\right)\alpha_i\left(\alpha_i\left(\sum_{m+n=j_1}\alpha_m\alpha_n\right)\right)\right)\end{aligned} \tag{16}$$

We notice that if $\alpha_1 = 0$ in Equation (16), then we can deduce from Equations (14) and (15) that $\alpha_k = 0$ ($k \in N^*$, $k \geq 1$), which is unreasonable.

Hence, we can consider that:

$$l^3 + (2\alpha d + 1)l^2 + (2\alpha d + \beta - \alpha)l + 2\alpha\beta d = 0 \tag{17}$$

where l is the eigenvalue of the characteristic polynomial of the chaotic system shown in Equation (4) evaluated at the equilibrium point O_3.

The following expression of α_k can be obtained from Equations (15) and (16):

$$\alpha_k = \frac{\alpha cr\left(2kl^2 i + kl + \beta\right)\left(3r\sum_{i+j=k}\alpha_i\alpha_j - \sum_{i+j_1=k}C_{con}\alpha_i\alpha_j\alpha_p\right)}{\omega(kl)} \tag{18}$$

where $\omega(kl) = kl^3 + (2\alpha d + 1)kl^2 + (2\alpha d + \beta - \alpha)lk + 2\alpha\beta d$, and C_{con} is a constant, $p \geq 1$.

Constrained by the first criterion of the Shilnikov method, we know that $\Delta > 0$, and Equation (2) has a unique negative root. Under this condition, $\omega(kl) \neq 0$, which determines the existence of α_k.

From Equations (15) and (16), α_k can be written as $\alpha_k = \varphi_k{\alpha_1}^k$, where φ_k is the family of functions depending on α, β, c, d, l.

The symmetry of Equation (11) points out that: if $x(t)$ is a solution for $t > 0$, then $-x(-t)$ is also a solution for $t < 0$, which means $\varphi(t)$ holds for $t < 0$.

Hence, $\varphi(t)$, the orbit of O_2 to O_3, takes the following form:

$$\varphi(t) = \begin{cases} -r + \sum\limits_{k=1}^{\infty}\alpha_k e^{klt}, & t > 0 \\ 0, & t = 0 \\ r - \sum\limits_{k=1}^{\infty}\alpha_k e^{-klt}, & t < 0 \end{cases} \tag{19}$$

The continuity and convergence of the series can be easily proved [33].

We can now confirm that there exists a heteroclinic orbit joining O_2 and O_3. The last thing that needs to be done is to prove in which condition the target system can satisfy the Shilnikov inequality $|\sigma/\gamma| < 1$.

For $\Delta > 0$, the solution of Equation (5) is:

$$\begin{cases} \gamma_1 = \sqrt[3]{-\frac{Q}{2} + \sqrt{\frac{\Delta}{4\times 27}}} + \sqrt[3]{-\frac{Q}{2} - \sqrt{\frac{\Delta}{4\times 27}}} \\ \sigma_1 = -\frac{1}{2}\left(\sqrt[3]{-\frac{Q}{2} + \sqrt{\frac{\Delta}{4\times 27}}} + \sqrt[3]{-\frac{Q}{2} - \sqrt{\frac{\Delta}{4\times 27}}}\right) \\ \omega_1 = \frac{\sqrt{3}}{2}\left(\sqrt[3]{-\frac{Q}{2} + \sqrt{\frac{\Delta}{4\times 27}}} + \sqrt[3]{-\frac{Q}{2} - \sqrt{\frac{\Delta}{4\times 27}}}\right) \end{cases} \tag{20}$$

Depending on this result, one real root and a pair of conjugate complex roots of Equation (4) can be obtained as follows:

$$\begin{cases} \gamma = -(1 + 2\alpha(d+1))/3 + \gamma_1 \\ \sigma \pm j\omega = -(1 + 2\alpha(d+1))/3 + \sigma_1 \pm j\omega_1 \end{cases} \tag{21}$$

We know that if the EDM deionization model has one negative real root, which means $\gamma < 0$, then for Equation (4), from the Caldan Formula, the following relational expression can be given as:

$$\gamma + \sigma + j\omega + \sigma - j\omega = -(1 + 2\alpha d) < 0 \tag{22}$$

Hence, $\gamma + 2\sigma < 0$. To ensure $|\sigma/\gamma| < 1$, it is required that $\gamma < 0$. This means that $\sigma_1 > (1 + 2\alpha d)/3$, or:

$$-\frac{1}{2}\left(\sqrt[3]{-\frac{Q}{2} + \sqrt{\frac{\Delta}{108}}} + \sqrt[3]{-\frac{Q}{2} - \sqrt{\frac{\Delta}{108}}}\right) > \frac{-(1 + 2\alpha d)}{3} \tag{23}$$

where Q, Δ, α, d is related to L_1, L_2, C_1, R_1, R_2.

Equation (23) can be defined as the second threshold condition that leads to chaos. Having a review of both in Equation (9) and in Equation (23), the two threshold conditions are both determined by the inherent characteristics of the EDM system. According to the Shilnikov theory, this means that the EDM system could evolve towardsSmale horseshoes chaos under the interaction between the inner variables of the EDM system.

3. Time Series Analysis of Autonomous Chaos

3.1. Data Source of Autonomous EDM Process

To further verify this theoretical conclusion, in the following section, the existence of autonomous chaos in the EDM process will be identified by experimental analysis orienting the deionization process. The NH7740B Fast Wire EDM Tool was used to perform machining on a 45# steel bar with the dimensions 100 × 100 × 30 mm as a workpiece. A 0.18 mm column of Mo was selected as the tool electrode, which was at a positive voltage with respect to the work piece. Commercially available water-based EDM oil was used as the dielectric medium. The power settings were as follows:on time 48 µs, P-ratio (is equal to off time/on time) 6, and number of power amplifier 3. The P-ratio index is the ratio of pulse-off time and pulse-on time. The number of the power amplifier is directly related to the values of the current. The settings of the major process parameters are summarized in Table 1.

Table 1. Process parameters.

Parameter	Values
Workpiece	No. 45 steel
Thickness	30 mm
Electrode tool (wire)	Mo (diameter 0.18 mm)
Wire Speed	11.8 ms^{-1}
Voltage	100 V
Dielectric medium	Water-based EDM oil
Pulse on time	48 µs
P-ratio	6
Power amplifier	3 (tool number)

The evolution and the gap states of the EDM system can be described by the fluctuation of the voltage time series, which contains rich information of feature variables related to EDM's chaotic nature [34]. The variation of pulses during the machining process were captured using the Tektronix TDS2024 of a 200-MHz bandwidth oscilloscope with a maximum sampling rate of 2 GSa/s, and the gap voltage was measured using a voltage probe. The timbase ofthe oscilloscope was 1ms, and the duration of each acquisition window was expected to be 10ms.Pulse identification and classification have been introduced by many researchers [35]. Basically, four electrical pulse types can be distinguished: normal spark discharge, arcs, short circuits, and open circuits. This paper will focus on the arc and spark discharge process. The types of spark discharge as well as arcs can be more precisely

analyzed and classified as: stable spark, unstable spark, stable arc, transient arc [36]. It has been mentioned that deionization evolves with no external excitation and can reflect the autonomy of the EDM system. From the perspective of dynamical systems, this paper treats the pulse-on process as a non-autonomous process and the pulse-off process as autonomous process. Validation experiments (carried out with the process parameters shown in Table 1) were conducted to record the time series of the four EDM sub-processes, namely unstable spark discharge, stable spark discharge, transient arc discharge, and stable arc discharge. To guarantee the validity of the results, the research in this paper extracted data that are around 60 percent of the peak value. The sample data is shown in Figure 3.

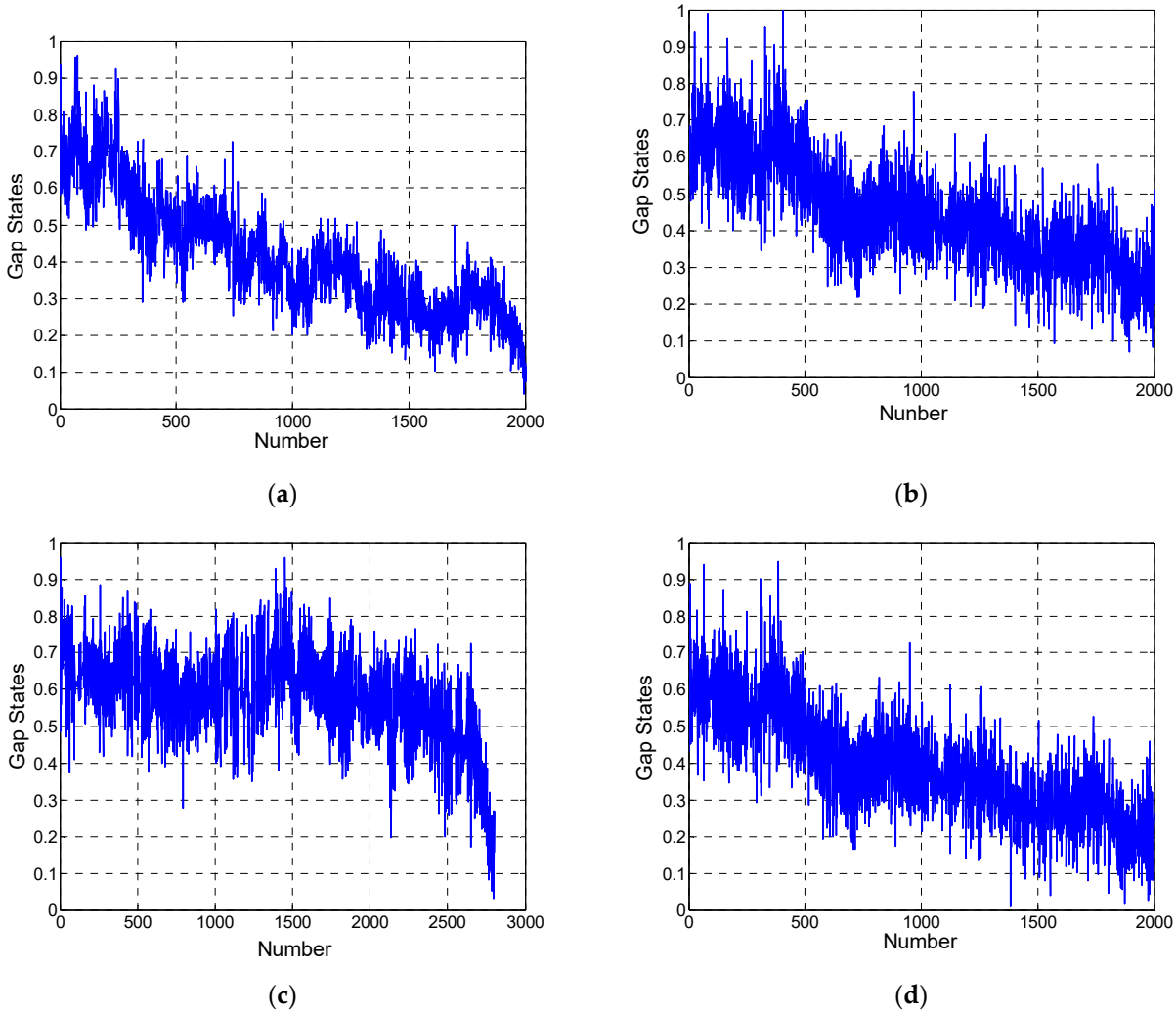

Figure 3. Gap states reflected autonomous EDM process. (**a**) Unstable spark discharge; (**b**) stable spark discharge; (**c**) stable arc discharge; (**d**) transient arc discharge.

3.2. Autonomous Chaotic Analysis Based on Qualitative Method

The results of the qualitative methods could be treated as necessary conditions for chaotic detection. For the purpose of chaotic feature extraction, commonly used appearance-based criteria include the power spectrum and the principal component spectrum [37,38].

The Power Spectrum Density (PSD) methodhas been used to investigate the EDM process. Marrocco et al. performed valuable research on the effective contribution of the normal discharge to the energy density at the operation frequency by using the Power Spectrum Density (PSD) method [39]. Zhou analyzed the deterministic nature of an efficient machining phase based on PSD analysis [25]. The calculation of the power spectrum in this paper implies the use of the classic PSD method. The power spectrum associated with

chaotic transitions is characterized by its broadband nature. The broadband nature refers to there being no obvious peaks on the power spectrum curve. In contrast, periodic and stochastic time series' power spectrograms always have discrete peaks at the harmonics (and sub-harmonics). In this paper, the periodogram method developed in the Matlab environment was applied, and the parameters were set as follows: the FFT number was equal to 2^14, the sampling frequency was equal to 20MHz, and the filter window was boxcar. Based on the sample data mentioned above, Figure 4 shows the analysis results of the power spectrum. It illustrates that no obvious peak could be found in the curves. Hence, all the autonomous processes' data of the four EDM sub-process may have chaotic characteristics. It should be mentioned that the power spectrum analysis is not sufficient to state the existence of chaos. If the system is in a multiple-period state, the power spectrum of its finite time series will have discrete peaks. However, the fact is that this system will finally evolve towards chaos [40]. In order to reach a valid conclusion, further analysis will be made.

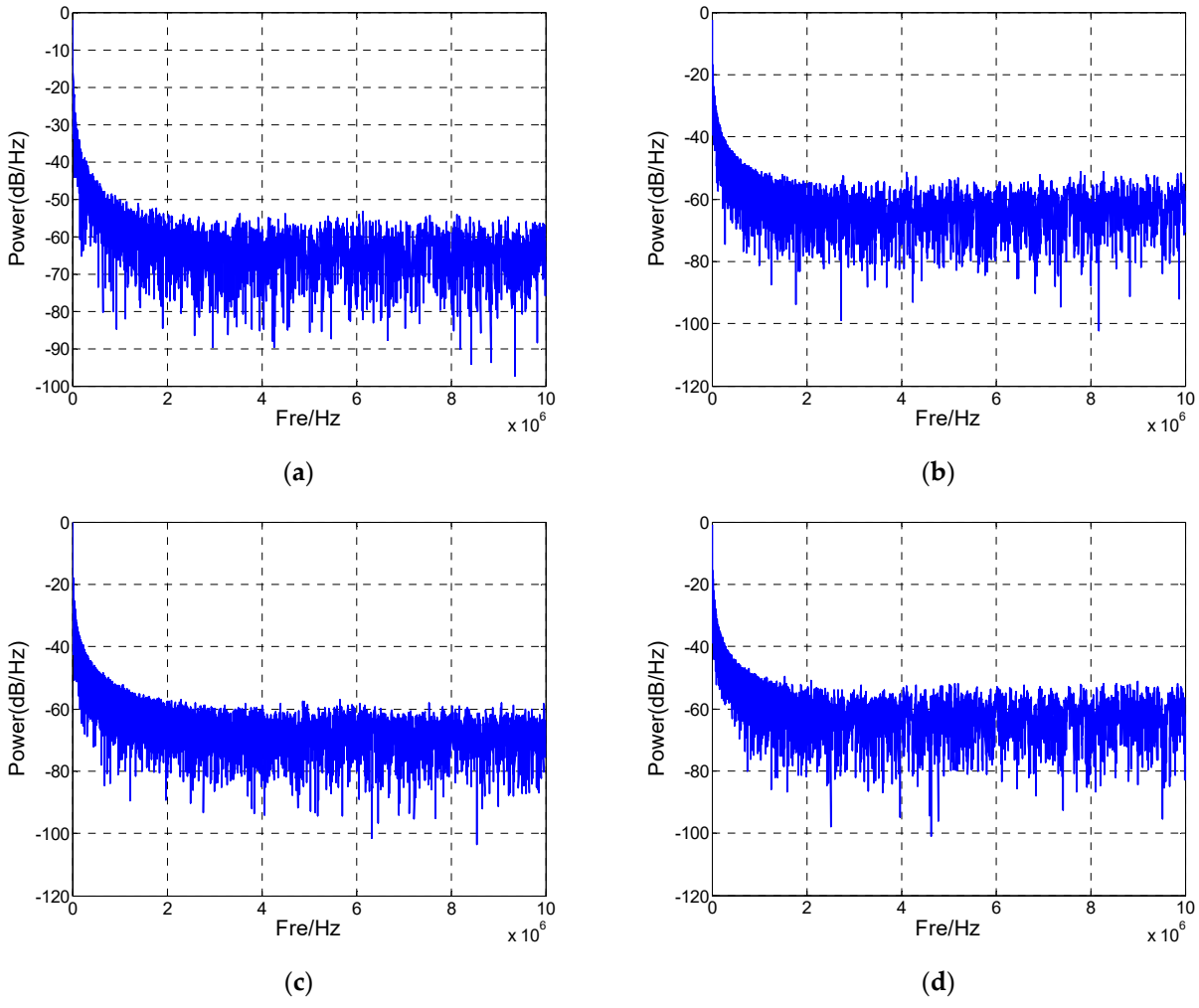

Figure 4. PSD of autonomous EDM process for pulse-on-time = 48 µs, p-ratio = 6, power-amplifier = 3. (**a**) Unstable sparkdischarge; (**b**) stable spark discharge; (**c**) stable arc discharge; (**d**) transient arc discharge.

Principal component analysis (PCA) is also an efficient method that can define the specific orthogonal projection basis and then reveal chaotic features from a qualitative perspective. The basic working principle of principal component analysis is to reduce the dimensionality of large databases. If the orbits of the chaotic attractor are defined as a collection of N point masses distributed in m-dimensional space, the principal components

are projections of associated state vectors onto the principal axes of inertia of such a mass distribution. Simply, if one time series can be regarded as a chaotic sequence, its principal component spectrogram should be able to fit a line within the negative slope.

Figure 5 is the principal component spectrum of four EDM sub-processes. Obviously, the curves could be regarded as straight lines with a negative slope. According to the principal component criterion, the autonomous EDM system has chaotic characteristics.

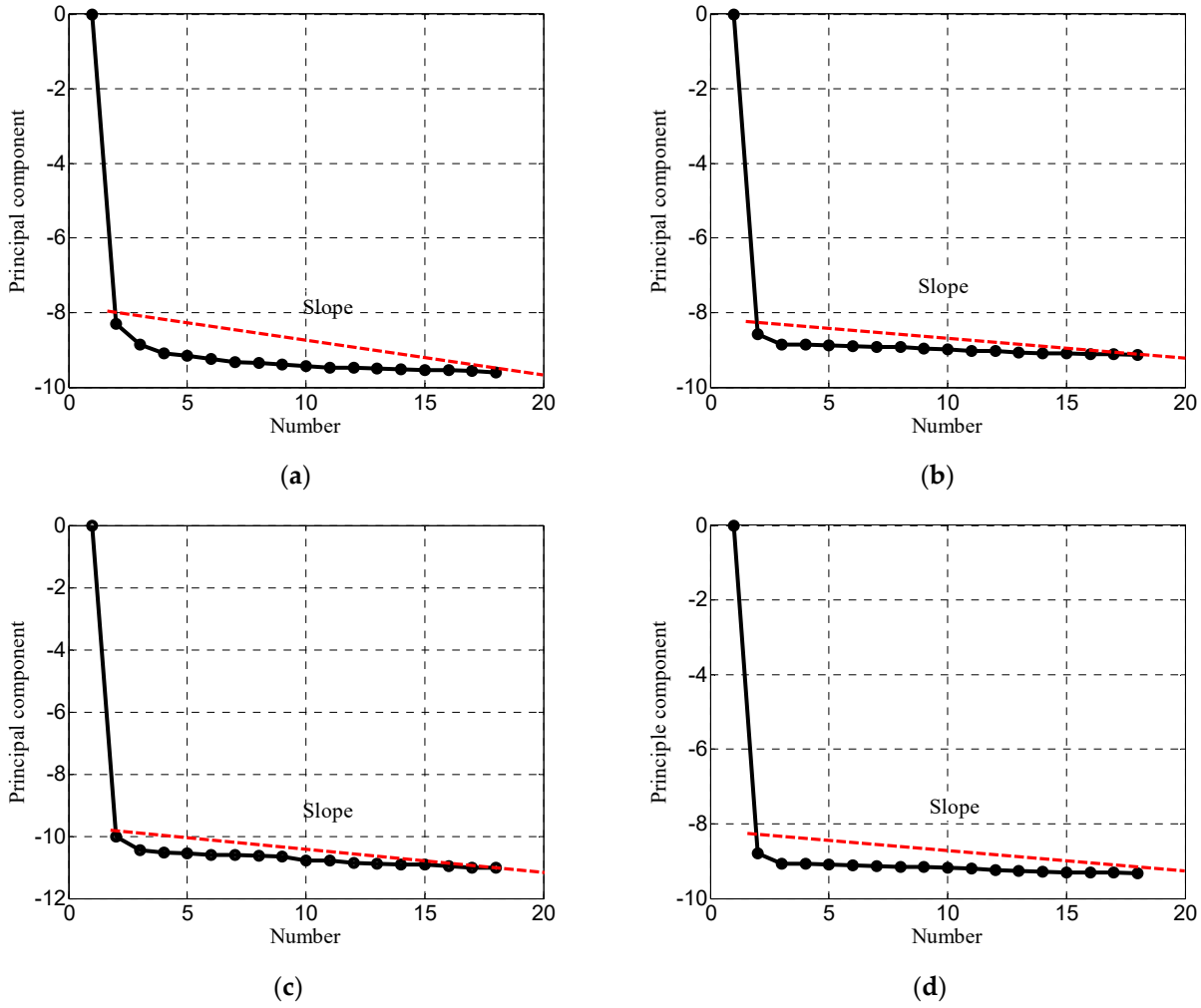

Figure 5. PCA of autonomous EDM process and the tendency of projections of associated state vectors onto the principal axes of inertia of such mass distribution. (**a**) Unstable spark discharge; (**b**) stable spark discharge; (**c**) stable arc discharge; (**d**) transient arc discharge.

3.3. Autonomous Chaotic Analysis Based on Quantitative Method

The saturated correlation dimension (SCD) and the largest Lyapunov exponent (LLE) are two efficient signatures of chaos [41,42]. This work calculates SCD to estimate the fractal dimension and uses LLE to distinguish the time series between stochastic and chaotic behaviors.

The concept of SCD methods is to measure degrees of freedom that are contributed by the movement of points lying on the attractor orbit. Based on the Grassberger and Procaccia (GP) theory [43], the SCD can be calculated by evaluating the stable slope of the curve of $\ln C_m(r)$ versus $\ln(r)$ for increasing values of m, wherer is a constant close to zero and misdefined as the embedded dimension. If the SCD is finite and non-integer, the system is considered to have chaotic behavior. Figure 6 shows the analytical results of the autonomous process. We can conclude that the SCD is 6.82 for unstable spark discharge, 6.30 for stable spark discharge, 5.89 for transient arc discharge, and 6.80 for stable arc

discharge. It was discovered that the autonomous EDM process saturates at a non-integer value at each discharge state and can be regarded as a chaotic system.

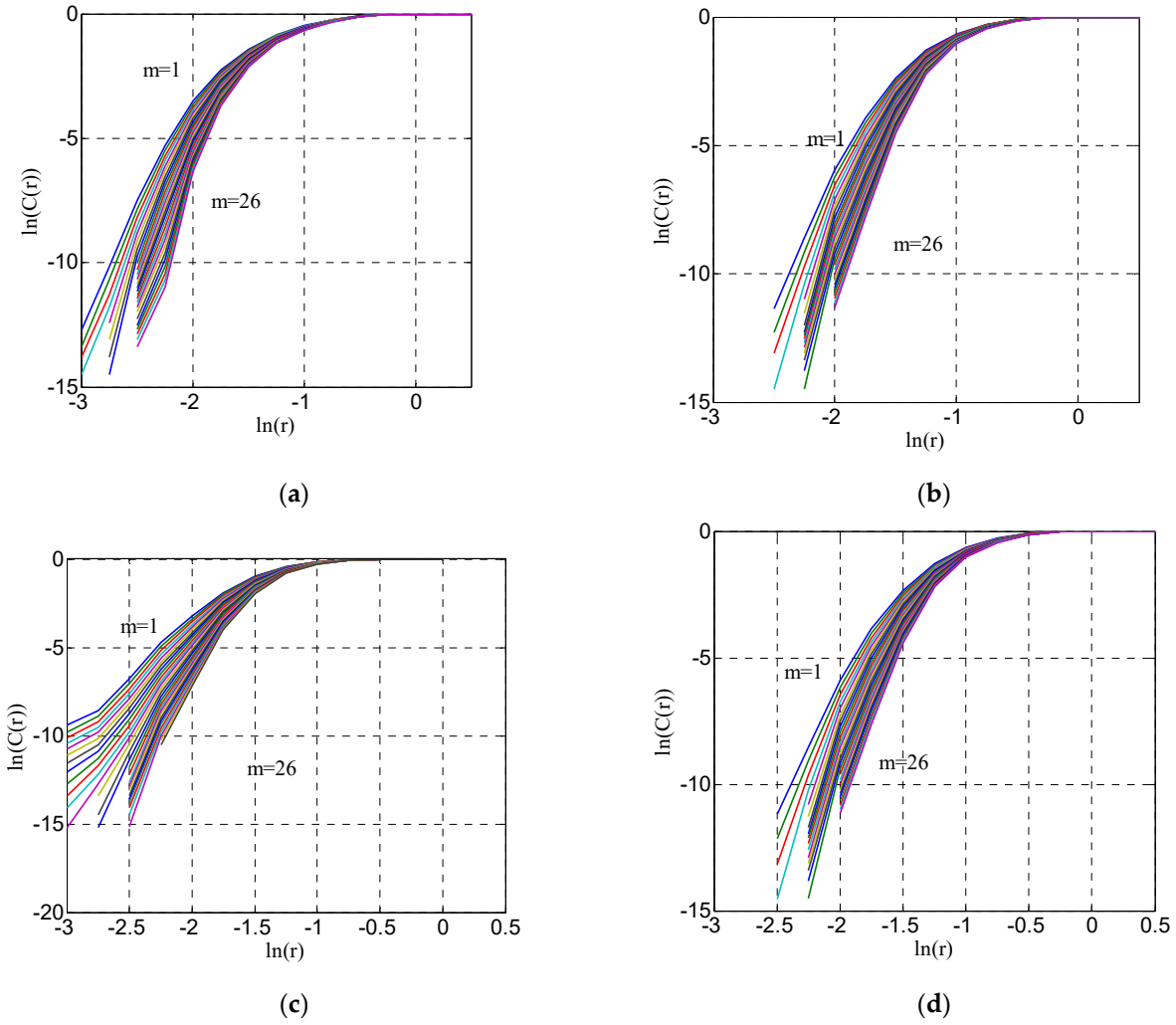

Figure 6. The distribution of $\ln C_m(r)$ versus $\ln(r)$ calculated by GP theory. (**a**) Unstable spark discharge; (**b**) stable spark discharge; (**c**) stable arc discharge; (**d**) transient arc discharge.

The essence of LLE is that chaotic behavior can be described by the exponential divergence of nearby orbits in phase space. For a chaotic and low-dimensional deterministic process, the LLE should be positive and finite. For a linear and limit cycle process, it should be zero. For a stochastic process, it should be either negative or infinite. Table 2 demonstrates that however much the data length changes, the LLE of the autonomous EDM process stays above zero. The LLE is 0.0027 for stable spark discharge, 0.0026 for unstable spark discharge, 0.0021 for transient arc discharge, and 0.0022 for stable arc discharge. According to LLE criterion, the positive and finite LLE means that the autonomous part of the EDM time-series presents ordinary chaotic behavior.

Table 2. Largest Lyapunov exponent of autonomous EDM process.

Data Length	StableSpark Discharge	Unstable Spark Discharge	Transient Arc Discharge	Stable Arc Discharge
500	0.0011	0.0022	0.0016	0.0020
800	0.0011	0.0026	0.0016	0.0021
1100	0.0027	0.0025	0.0019	0.0022
1500	0.0023	0.0025	0.0021	0.0020
2000	0.0027	0.0026	0.0019	0.0022

4. Discussion

As mentioned above, the pulse-on EDM process can be treated as a non-autonomous system, and its chaotic behavior has been studied theoretically and experimentally. Gatto et al. [24] found chaos in the EDM discharging process and theoretically used the logistic map recursive equation to describe the energy evolution in the non-autonomous process. Zhou et al. [25] applied the surrogate data method to analyze the chaotic behavior of the efficient machining process. In our previous work, we established a mathematical model and used the Melnikov theory to evaluate the threshold condition of non-autonomous EDM behavior and provide experimental evidence. In this section, we compare the quantitative results of the autonomous EDM process with the non-autonomous EDM process to investigate the chaotic dynamical mechanism of the overall EDM process. Table 2 consists of the LLEs of six sets of experimental data, which sufficiently denotes obvious variations of positive LLE when changing the EDM discharge channel from a non-autonomous discharge duration to an autonomous deionization duration. Based on the above analysis, we confirm that both the autonomous and non-autonomous EDM process have dynamical chaotic characteristics.

Figure 7 illustrates the distribution of the relationship between LLE and SCD, which shows that, under different electrical discharge sub-processes, the fitting circular area of the autonomous EDM process is not coincident with, but could be even larger than the non-autonomous EDM process. We can conclude that the EDM system sustains chaotic dynamical evolution in the whole machining cycle.

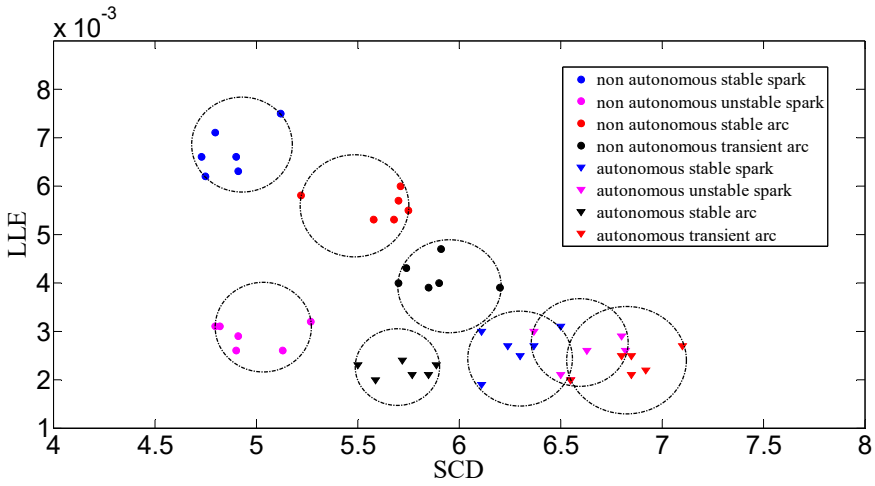

Figure 7. The distribution of relationship between LLE and SCD.

This conclusion is consistent with the results of previous works. Hayakawa observed that the chemical–physical reaction would be persistent in the deionization duration and reported that the dimension of debris particles in the deionization duration is larger than the dimension in the discharge duration [44]. Gatto et al. [24] defined a pulse-on time and a pause time (corresponding to this paper's autonomous process and non-autonomous process, respectively) as one complete EDM cycle and conjectured that the variation of free energy is chaotic in each EDM cycle. As shown in Figure 7 and Table 3, it can also be

observed that the variation of LLE in the autonomous process is relatively more stable. A deduction could be made that the EDM system evolves towards steady chaos without an external intervention.

Table 3. Largest Lyapunov exponent of 6 sets of experiment data [1].

Set	Stable Spark Discharge		Unstable Spark Discharge		Transient Arc Discharge		Stable Arc Discharge	
	NA	A	NA	A	NA	A	NA	A
1	0.0066	0.0025	0.0026	0.0026	0.0053	0.0023	0.0039	0.0025
2	0.0075	0.0027	0.0032	0.0021	0.0060	0.0021	0.0047	0.0024
3	0.0066	0.0030	0.0026	0.0029	0.0053	0.0023	0.0039	0.0027
4	0.0062	0.0031	0.0029	0.0020	0.0058	0.0020	0.0040	0.0021
5	0.0063	0.0027	0.0031	0.0026	0.0057	0.0021	0.0043	0.0022
6	0.0071	0.0019	0.0031	0.0030	0.0055	0.0024	0.0040	0.0025

[1] (A and NA are short for autonomous and non-autonomous).

5. Conclusions

This paper brings forward evidence of autonomous chaos in the EDM process.The conclusion introduces new knowledge for a better understanding of the deterministic nature of the EDM process and provides a deterministic nonlinear perspective for modeling a complete EDM process.

Theoretical analysis indicates that the autonomous dynamics in EDM are closely related to a Shilnikovhomoclinic chaos. A nonlinear equivalent model without external incentive is established to describe the autonomous EDM process. Two threshold conditions are obtained by the Shilnikov criteria. A conclusion is made that the EDM system can lead to autonomous chaos under the threshold conditions.

Experimental results are gathered to make a further verification. Confirmatory experiments are implemented, and time series recorded in the deionization process are analyzed by power spectrum analysis, principal component spectrum analysis, SCD analysis, and LLE analysis, to sufficiently prove the existence of autonomous chaos in the EDM process.

The quantitative results of the overall EDM process (including the autonomous and non-autonomous EDM process) are analyzed, and a deduction is made that the EDM system will evolve towards steady chaos under an autonomous state.

As potential applications, controlling autonomous chaos of EDM could be expected to minimize the deionization duration and ultimately energy loss in the machining process. The chaos control method can be a new way to improve machining efficiency.

Author Contributions: Conceptualization, P.W.; methodology, B.-H.L.; validation, P.W.; writing—original draft preparation, P.W.; writing—review and editing, B.W.; supervision, L.W.; funding acquisition, Z.W. All authors have read and agreed to the published version of the manuscript.

Funding: This research was funded by the National Natural Science Foundation of China (NNSFC, Contract name: Research on ultimate bearing capacity and parametric design for the grouted clamps strengthening the partially damaged structure of jacket pipes, grant number 51879063) and by the Interdisciplinary Foundation of BIPT (grant number 21032205004/005).

Institutional Review Board Statement: Not applicable.

Informed Consent Statement: Not applicable.

Data Availability Statement: Not applicable.

Conflicts of Interest: The authors declare no conflict of interest.

References

1. Balanou, M.; Karmiris-Obratański, P.; Leszczyńska-Madej, B.; Papazoglou, E.L.; Markopoulos, A.P. Investigation of surface modification of 60CrMoV18-5 steel by EDM with Cu-ZrO2 powder metallurgy green compact electrode. *Machines* **2021**, *9*, 268. [CrossRef]
2. Pachaury, Y.; Tandon, P. An overview of electric discharge machining of ceramics and ceramic based composites. *J. Manuf. Process.* **2017**, *25*, 369–390. [CrossRef]
3. Sanchez, J.A.; Cabanes, I.; Lopez de Lacalle, L.; Iamikiz, A. Development of optimum electrodischarge machining technology for advanced ceramics. *Int. J. Adv. Manuf. Technol.* **2001**, *18*, 897–905. [CrossRef]
4. DiBitonto, D.D.; Eubank, P.T.; Patel, M.R.; Barrufet, M.A. Theoretical models of the electrical discharge machining process. I. A simple cathode erosion model. *J. Appl. Phys.* **1989**, *66*, 4095. [CrossRef]
5. Patel, M.R.; Barrufet, M.A.; Eubank, P.T.; DiBitonto, D.D. Theoretical models of the electrical discharge machining process. II. The anode erosion model. *J. Appl. Phys.* **1989**, *66*, 4104. [CrossRef]
6. Eubank, P.T.; Patel, M.R.; Barrufet, M.A. Theoretical models of the electrical discharge machining process. III. The variable mass, cylindrical plasma model. *J. Appl. Phys.* **1993**, *73*, 7900. [CrossRef]
7. Teitsworth, S.W.; Westervelt, R.M.; Haller, E.E. Nonlinear oscillations and chaos in electrical breakdown in Ge. *Phys. Rev. Lett.* **1983**, *51*, 825–828. [CrossRef]
8. Alisultanov, Z.Z.; Ragimkhanov, G.B. Fractional-differential approach to the study of instability in a gas discharge. *ChaosSolitons Fractals* **2018**, *107*, 39–42. [CrossRef]
9. Allagui, A.; Rojas, A.E.; Bonny, T.; Elwakil, A.S.; Abdelkareem, M.A. Nonlinear time-series analysis of current signal in cathodic contact glow discharge electrolysis. *J. Appl. Phys.* **2016**, *119*, 203303. [CrossRef]
10. Braun, T.; Lisboa, J.A.; Gallas, J.A.C. Evidence of homoclinic chaos in the plasma of a glow discharge. *Phys. Rev. Lett.* **1992**, *68*, 2770–2773. [CrossRef] [PubMed]
11. Braun, T.; Lisboa, J.A.; Francke, R.E.; Gallas, J.A. Observation of deterministic chaos in electrical discharges in gases. *Phys. Rev. Lett.* **1987**, *59*, 613. [CrossRef]
12. Zhang, D.Z.; Wang, Y.H.; Wang, D.Z.H. Numerical study on the discharge characteristics and nonlinear behaviors of atmospheric pressure coaxial electrode dielectric barrier discharges. *Chin. Phys. B* **2017**, *6*, 263–269. [CrossRef]
13. Nielsen, A.H.; Pécseli, H.L.; Rasmussen, J.J. Turbulent transport in low-β plasmas. *Phys. Plasmas* **1996**, *3*, 1530–1544. [CrossRef]
14. Carreras, B.A.; Milligen, V.; Pedrosa, M.A.; Balbín, R.; Hidalgo, C.; Newman, D.E.; Sánchez, E.; Frances, M.; García-Cortés, I.; Bleuel, J.; et al. Self-similarity of the plasma edge fluctuations. *Phys. Plasmas* **1998**, *5*, 3632–3643. [CrossRef]
15. Carreras, B.A.; van Milligen, B.; Hidalgo, C.; Balbin, R.; Sanchez, E.; Garcia-Cortes, I.; Pedrosa, M.A.; Bleuel, J.; Endler, M. Self-similarity properties of the probability distribution function of turbulence-induced particle fluxes at the plasma edge. *Phys. Rev. Lett.* **1999**, *83*, 3653. [CrossRef]
16. Cheung, P.Y.; Wong, A.Y. Chaotic behavior and period doubling in plasmas. *Phys. Rev. Lett.* **1987**, *59*, 551–554. [CrossRef]
17. Cheung, P.Y.; Donovan, S.; Wong, A.Y. Observations of intermittent chaos in plasmas. *Phys. Rev. Lett.* **1988**, *61*, 1360–1363. [CrossRef] [PubMed]
18. Wilson, R.B.; Podder, N.K. Observation of period multiplication and instability in a dc glow discharge. *Phys. Rev. E* **2007**, *76*, 046405. [CrossRef] [PubMed]
19. Lahiri, S.; Roychowdhury, D.; SekarIyengar, A.N. Long range temporal correlation in the chaotic oscillations of a dc glow discharge plasma. *Phys. Plasmas* **2012**, *19*, 082313. [CrossRef]
20. Nurujjaman, M.; Narayanan, R.; SekarIyengar, A.N. Parametric investigation of nonlinear fluctuations in a dc glow discharge plasma. *Chaos* **2007**, *17*, 170. [CrossRef] [PubMed]
21. Ohno, N.; Tanaka, M.; Komori, A.; Kawai, Y. Chaotic behavior of current-carrying plasmas in external periodic oscillations. *J. Phys. Soc. Jpn.* **1989**, *58*, 28–31. [CrossRef]
22. Han, F.; Kunieda, M. Chaos found in distribution of EDM spark. In Proceedings of the 13th International Symposium for Electromachining ISEM XIII, Bilbao, Spain, 9–11 May 2001; pp. 185–192.
23. Aich, U.; Banerjee, S. Evaluation for chaos in EDM generated surface topography. *KEM* **2018**, *765*, 227–231.
24. Gatto, A.; Sofroniou, M.; Spaletta, G.; Bassoli, E. On the chaotic nature of electro-discharge machining. *Int. J. Adv. Manuf. Technol.* **2015**, *79*, 985–996. [CrossRef]
25. Zhou, M.; Han, F.Z.H.; Wang, Y.X.; Soichiro, I. Assessment of the dynamical properties in EDM process-detecting deterministic nonlinearity of EDM process. *Int. J. Adv. Manuf. Technol.* **2009**, *44*, 91–99. [CrossRef]
26. Wang, P.; Li, B.; Shi, G.; Lin, T.; Wang, B.X. Non-linear mechanism in electrical dischargemachining process. *Int. J. Adv. Manuf. Technol.* **2018**, *97*, 1687–1696. [CrossRef]
27. Fonseca, J.; Marafona, J.D. The effect of deionisation time on the electrical discharge machining performance. *Int. J. Adv. Manuf. Technol.* **2014**, *71*, 471–481. [CrossRef]
28. Hayakawa, S.; Sasaki, S.; Itoigawa, F.; Nakamura, T. Relationship between occurrence of material removal and bubble expansion in electrical discharge machining. *Procedia CIRP* **2013**, *6*, 174–179. [CrossRef]
29. Hayakawa, S.; Kusafuka, Y.; Itoigawa, F.; Nakamura, T. Observation of material removal from discharge spot in electrical discharge machining. *Procedia CIRP* **2016**, *42*, 12–17. [CrossRef]
30. Colpo, P. Determination of the equivalent circuit of inductively coupled plasma sources. *J. Appl. Phys.* **1999**, *85*, 1366. [CrossRef]

31. Valery, A.; Godyak, R.B.P.B. Electrical characteristics of parallel-plate RF discharges in Argon. *IEEE Transac. Plasma Sci.* **1991**, *19*, 4.
32. Arneodo, A.; Coullet, P.; Tresser, C. Oscillators with chaotic behavior: An illustration of a theorem by shil'nikov. *J. Stat. Phys.* **1982**, *27*, 171–182. [CrossRef]
33. Sun, F.Y. Shil'nikovheteroclinic orbits in a chaotic system. *Int. J. Mod. Phys. B* **2007**, *21*, 4429–4436. [CrossRef]
34. Zhou, Y.; Zhu, H.; Zuo, X.; Yang, J. Chaotic characteristics of measured temperatures during sliding friction. *Wear* **2014**, *317*, 17–25. [CrossRef]
35. Modica, F.; Guadagno, G.; Marrocco, V.; Fassi, I. Evaluation of micro-EDM milling performance using pulse discrimination. In Proceedings of the International Design Engineering Technical Conferences and Computers and Information in Engineering Conference, Buffalo, NY, USA, 17–20 August 2014.
36. Dauw, D.F.; Snoeys, R.; Dekeyser, W. Advanced pulse discriminating system for EDM process analysis and control. *CIRP Annals* **1983**, *32*, 541–549. [CrossRef]
37. Gollub, J.P.; Swinney, H.L. Onset of turbulence in a rotating fluid. *Phys. Rev. Lett.* **1975**, *35*, 927. [CrossRef]
38. Vojnović, B.; Michieli, I. Detecting noise in chaotic signals through principal component matrix transformation. *J. Comput. Inf. Tech.* **2003**, *11*, 55–66.
39. Marrocco, V.; Modica, F.; Fassi, I. Analysis of discharge pulses in micro-EDM milling of Si3N4-TiN composite workpiece by means of power spectral density (PSD). *J. Manuf. Process.* **2019**, *43*, 112–118. [CrossRef]
40. Li, T.Y.; Yorke, J.A. Period three implies chaos. *Am. Math. Mon.* **1975**, *82*, 985–992. [CrossRef]
41. Fan, X.; Li, S.; Tian, L. Chaotic characteristic identification for carbon price and an multi-layer perceptron network prediction model. *Expert. Syst. Appl.* **2015**, *42*, 3945–3952. [CrossRef]
42. Silva, R.; Araújo, A. The Deterministic nature of sensor-based information for condition monitoring of the cutting process. *Machines* **2021**, *9*, 270. [CrossRef]
43. Grassberger, P.; Procaccia, I. Measuring the strangeness of strange attractors. *Physica D* **1983**, *9*, 189–208. [CrossRef]
44. Hayakawa, S.; Minoura, K.; Itoigawa, F.; Nakamura, T. Study on material removal mechanism in EDM process through observation of resolidification of molten metal. *Procedia CIRP* **2018**, *68*, 266–271. [CrossRef]